Available online at www.sciencedirect.com

ScienceDirect

Solar Energy 84 (2010) 501–506

SOLAR ENERGY

www.elsevier.com/locate/solener

Estimation of total cloud cover from solar radiation observations at Lake Rotorua, New Zealand

Liancong Luo [a,b,*], David Hamilton [a], Boping Han [c]

[a] Centre of Biodiversity and Ecology Research, Waikato University, Private Bag 3105, Hamilton 3240, New Zealand
[b] State Key Laboratory of Lake Science and Environment, Nanjing Institute of Geography and Limnology, Chinese Academy of Sciences, Nanjing 210008, PR China
[c] Research Centre of Hydrobiology, Department of Ecology, Jinan University, Guangzhou 510632, PR China

Received 15 May 2009; received in revised form 31 December 2009; accepted 11 January 2010

Communicated by: Associate Editor Frank Vignola

Abstract

The DYRESM-CAEDYM model is a valuable tool for simulating water temperature for biochemical studies in aquatic ecosystem. The model requires inputs of surface short-wave radiation and long-wave radiation or total cloud cover fraction (*TC*). Long-wave radiation is often not measured directly so a method to determine *TC* from commonly measured short-wave solar irradiance (E_0) and theoretical short-wave solar irradiance under a clear sky (E_c) has broad application. A more than 17-year (15 November 1991 to 20 February 2009) hourly solar irradiance data set was used to estimate the peak solar irradiance for each ordinal date over one year, which was assumed to be representative of solar irradiance in the absence of cloud. Comparison between these daily observed values and the modelled clear-sky solar radiation over one year was in close agreement (Pearson correlation coefficient, $r = 0.995$ and root mean squared error, $\mathrm{RMSE} = 12.54\ \mathrm{W\ m^{-2}}$). The downloaded hourly cloudiness measurements from 15 November 1991 to 20 February 2009 was used to calculate the daily values for this period and then the calculated daily values over the 17 years were used to calculate the average values for each ordinal date over one year. A regression equation between $(1 - E_0/E_c)$ and *TC* produced a correlation coefficient value of 0.99 ($p > 0.01$, $n = 71$). The validation of this cloud cover estimation model was conducted with observed short-wave solar radiation and *TC* at two sites. Values of *TC* derived from the model at the Lake Rotorua site gave a reasonable prediction of the observed values ($\mathrm{RMSE} = 0.10$, $r = 0.86$, $p > 0.01$, $n = 61$). The model was also tested at Queenstown (South Island of New Zealand) and it provided satisfactory results compared to the measurements ($\mathrm{RMSE} = 0.16$, $r = 0.67$, $p > 0.01$, $n = 61$). Therefore the model's good performance and broad applicability will contribute to the DYRESM-CAEDYM accuracy of water temperature simulation when long-wave radiation is not available.

Keywords: Clear-sky solar irradiance; DYRESM-CAEDYM; Long-wave radiation

1. Introduction

The one-dimensional water quality model (DYRESM-CAEDYM) is commonly used to simulate water temperature, salinity, density and water quality in lakes and reservoirs (Hamilton and Schladow, 1997; Schladow and Hamilton, 1997; Gal et al., 2003). The hydrodynamic model (DYRESM) is based on a Lagrangian architecture that models a lake as a series of horizontal layers with uniform properties (e.g., temperature and salinity; Romero et al., 2004). It uses heat balance equations to determine water temperature within each of the water layers. Surface exchanges are responsible for the majority of the energy for

* Corresponding author. Address: State Key Laboratory of Lake Science and Environment, Nanjing Institute of Geography and Limnology, Chinese Academy of Sciences, Nanjing 210008, PR China.
E-mail addresses: lluo@waikato.ac.nz, lcluo@niglas.ac.cn (L. Luo).

0038-092X/$ - see front matter © 2010 Published by Elsevier Ltd.
doi:10.1016/j.solener.2010.01.012

heating, mixing and stratifying the lake. These exchanges include heating due to short-wave radiation penetration into the lake, latent heat (i.e., evaporative cooling), sensible heat (i.e., convection of heat between the water surface and the atmosphere), long-wave radiation and wind stress (Gal et al., 2003). Short-wave radiation (waveband 280–2800 nm) is usually measured directly whilst long-wave radiation (waveband >2800 nm) may also be measured directly as an incident or net value, or indirectly from cloud cover, air temperature and humidity (Tennessee Valley Authority, 1972). Direct and indirect long-wave radiation measurements are often not available due to the expense and maintenance required for these instruments. Cloud cover, therefore, is used as the only remaining alternative for long-wave input data to DYRESM-CAEDYM, together with air temperature and humidity.

There are two methods commonly used to estimate cloud cover. One is based on ground observations (Kasten and Czeplak, 1980; Calbo, 2001; Kim and Hofmann, 2005) and the other is based on satellite mounted sensors or digital cameras (Sospedra et al., 2004; Yamashita et al., 2004; Richards and Sullivan, 2009). In the first method, cloud cover is calculated from observed short-wave solar irradiance, together with theoretical solar irradiance with clear sky. The second uses the colour strength of images and retrieval models to compute cloudiness. Satellites are able to observe unexplored or unmonitored areas of Earth, but the measurements obtained from onboard satellite sensors are not as accurate as surface measurements due to the technical limits of observational sensors and retrieval errors. Furthermore, a large volume of satellite data is required to be collected, evaluated, and analyzed. Ground observational radiation data, therefore, are often used for cloud cover calculations.

A wide range of retrieval models for cloud cover estimation have previously been developed, based on ground observations (Kasten and Czeplak, 1980; Davis, 1995; Kim and Hofmann, 2005). In most of the models, the ratio of observed (E_0) to clear-sky solar radiation (E_c) is used to compute fractional cloud cover. Cloudiness increases with a decrease in the value of E_0/E_c. For example, Kasten and Czeplak (1980) formulated an equation of E_0/E_c as a function of cloud cover to the power of 3.4. This model was then modified by Gul et al. (1998) and Muneer and Gul (2000), with a change in the value of the exponent. Younes and Muneer (2007) discussed other models for cloud cover estimation methods but found that Kasten and Czeplak's model was one of the best models in terms of statistical performance.

In this paper, we use a simple solar broadband model (Bird and Hulstrom, 1981; Bird, 1984; Bird and Riordan, 1986) to calculate the global irradiance on a horizontal surface under a clear sky in the Lake Rotorua district of New Zealand. The computed clear-sky irradiance was then used to calculate E_0/E_c with solar irradiance measurements. Based on the observed cloudiness, we developed a regression relationship between E_0/E_c and total cloud cover (*TC*). The regression equation was then used to estimate *TC*, thereby providing suitable input data for determining long-wave radiation heat fluxes in DYRESM-CAEDYM, in the absence of direct measurements of total or net long-wave radiation data.

2. Methodology

2.1. Clear-sky irradiation simulation model

Global horizontal radiation under a clear sky was calculated from the Bird Clear-Sky Model (BCSM, Bird and Hulstrom, 1981) modified further as the SPCTRAL2 model (Bird, 1984; Bird and Riordan, 1986). This model predicts clear-sky direct beam, hemispherical diffuse, and total hemispherical broadband solar radiation on a horizontal surface. Average solar radiation is computed hourly with 10 user-specified input parameters. However, variable atmospheric parameters such as aerosol optical depth (AOD), ozone and water vapour are held constant for the entire year (Bird and Hulstrom, 1981). Karalis et al. (1982) compared this model to two other theoretical models proposed by Davies-Hay and Hoyt and found that it gave very good results for global solar irradiance and direct irradiance for most of the months of the simulation year especially in winter and spring months. But even in summer months the relative error is not greater than 12.0% except for the early morning hours.

The basic equations for direct (I_d), diffuse (I_{as}) and global irradiance (I_T) are given as (Bird and Hulstrom, 1981; Bird, 1984; Bird and Riordan, 1986)

$$I_d = I_0(\cos z)(0.9662)T_rT_aT_wT_oT_{um} \tag{1}$$

$$I_{as} = I_0(\cos z)(0.79)T_{aa}T_wT_oT_{um} \tag{2}$$

$$I_T = (I_d + I_{as})/(1 - r_g r_s) \tag{3}$$

Here I_0, I_d, I_{as}, and I_T are the extraterrestrial solar irradiance (1367 W m^{-2}), the direct solar irradiance, the solar irradiance from atmospheric scattering and the total (global) solar irradiance on a horizontal surface. The parameters z, T_r, T_a, T_{aa}, T_w, T_o, T_{um} represent the solar zenith, transmittances of Rayleigh scattering, aerosol absorptance and scattering, and the absorptances of aerosols, water vapour, ozone and uniformly mixed gases (carbon dioxide and oxygen), respectively. The remaining parameters are r_g, the ground albedo (0.2, Karalis et al., 1982), and r_s, the sky/atmospheric albedo given by:

$$r_s = 0.0685 + (1 - 0.84)(1 - T_a/T_{aa}) \tag{4}$$

The key input parameters for the model are shown in Table 1.

Precipitable water (W, unit in cm) is calculated based on its logarithm relationship with dew temperature (°C) at Auckland which is about 200 km away from Lake Rotorua (Tuller, 1977). It can be expressed as,

$$\mathrm{In}(W) = a \times T_d + b \tag{5}$$

Table 1
Key input parameters for the solar radiation model.

Parameters	Units	Value
Mean solar constant	$W\ m^{-2}$	1367
Longitude	Degrees (West is "−")	176.32
Latitude	Degrees (North is " + ")	−38.11
Sea level pressure	hPa	1010
Surface albedo	Dimensionless	0.2

where W is precipitable water (cm) and T_d is dew point temperature (°C), a is a constant regression coefficient (0.09 spring, 0.07 summer and autumn, 0.08 winter), b is the regression constant (1.88 spring, 2.11 summer, 2.12 autumn and 2.01 winter).

Monthly ozone (DU) at Lauder, New Zealand were obtained from National Oceanic and Atmospheric Administration (Oltmans et al., 2009). The monthly values are shown in Table 2. The missing value in February was calculated as the average between January and March. The produced daily precipitable water data through the year are shown in Fig. 1.

Monthly AOD at 500 nm was measured from February 1996 to May 1997 and from August 1999 to December 2008. Average monthly AOD at 500 nm through the year (ordinal date from 1 to 366) was calculated using these measurements. AOD at 380 nm was not available but monthly AOD at 368 nm was recorded from February 1996 to May 1997. We have found AOD at different wavelengths (i.e., 368 nm, 412 nm, 500 nm and 674 nm) show similar patterns of seasonal variation, therefore, we calculated monthly AOD at 380 nm as the average of AOD at 500 nm and 368 nm. The monthly ozone and AOD at 500 nm and 380 nm are shown in Table 2.

2.2. Data preparation and cloudiness estimation

Observed hourly solar radiation and cloudiness data were obtained from the climate database of National Institute of Water and Atmospheric Research, New Zealand (NIWA) for the period 15 November 1991 – 20 February 2009. We calculated hourly data, daily data and Julian time for observed data with a time interval of 15 min. During the period when data were unavailable (e.g. sensor malfunction), a linear interpolation was used to fill the blanks based on the available measurements.

We used correlations between measurements of solar irradiance and cloud fraction to develop a model that can be used to predict cloud fraction from solar irradiance when cloud fraction measurements are not available. Based on the measured solar radiation and cloud cover downloaded from NIWA, we calculated the fractional cloud cover with the following six steps.

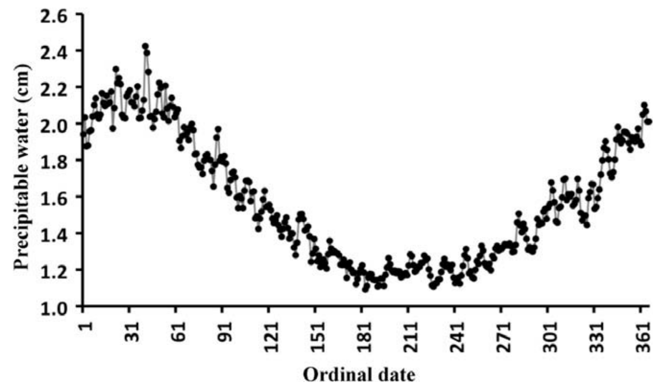

Fig. 1. Calculated daily precipitable water (cm) through the year (1–366).

(1) Convert the hourly octa cloud value to a fractional value ranging from 0 to 1 for the low, middle and high layers (i.e., division by 8).
(2) Calculate daily values of solar radiation and cloudiness based on the hourly data.
(3) Calculate theoretical solar radiation (i.e., clear sky) for each day of the year, based on the Bird model, using input data shown in Table 1.
(4) Calculate the daily solar fraction (observed solar radiation divided by theoretical solar radiation).
(5) Sort the daily cloudiness fraction into 74 bins corresponding to intervals of 0.01 in the range 0.0–0.73 (no value greater than 0.73). Calculate the average solar fraction value for each data bin.
(6) Regress $(1 - E_0/E_c)$ with TC after deleting the abnormal data.

Based on the calculated daily solar radiation from 15 November 1991 to 20 February 2009, a peak value for each day of the year was then used to represent clear-sky solar radiation for each day, for comparison with the theoretical model output. The total cloud cover was then computed as (Marion and George, 2001):

$$TC = (T_l + T_m + T_h)/3.0 \tag{6}$$

The variables TC, T_l, T_m and T_h are the fractional total cloud cover, and low (Cirrocumulus), middle (Cirrostratus) and high-layer (Altocumulus) cloud cover, respectively, in the range of 0.0–1.0.

Table 2
Monthly mean total ozone amounts (cm), AOD at 500 nm (AOD500, in cm) and AOD at 380 nm (AOD380, in cm).

Month	January	February	March	April	May	June	July	August	September	October	November	December
Ozone	0.279	–	0.265	0.271	0.276	0.297	0.306	0.324	0.324	0.326	0.317	0.299
AOD500	0.033	0.027	0.022	0.021	0.018	0.017	0.019	0.023	0.034	0.033	0.030	0.028
AOD380	0.038	0.035	0.027	0.024	0.024	0.019	0.022	0.026	0.037	0.034	0.031	0.032

3. Results

3.1. Comparison of simulated clear-sky solar irradiance with observations

Peak values of solar irradiance for each ordinal date (1–366) were established from observed data for the period 15 November 1991 – 20 February 2009. A comparison of observations with daily values simulated by the model shows good agreement, with both measured and modelled daily values within the range 103.6 (winter) to 387.7 (summer) W m^{-2} (Fig. 2). The root mean squared error (RMSE) of the comparison is 12.54 W m^{-2} and the Pearson correlation coefficient (r) is 0.995. The simulation tends to overestimate observations slightly, which may reflect the fact that despite 17 years of data, the assigned daily peak over one year may still, in some cases, have been influenced by cloud cover.

3.2. Cloudiness regression

There is a large body of literature addressing the relationship between the ratio of observed solar radiation to clear-sky solar radiation (E_0/E_c) and total cloud cover (TC). Most relationships take the form (Kasten and Czeplak, 1980; Davis, 1995; Kim and Hofmann, 2005):

$$\frac{E_0}{E_c} = 1.0 - a \cdot TC^b \tag{7}$$

Here a and b are constants produced from regression relationships. Using Eq. (7), we developed a regression relationship, taking the form of a polynomial cubic equation, to estimate the cloudiness fraction, which is given as (Fig. 3),

$$\frac{E_0}{E_c} = 1 - 1.9441 \cdot TC^3 + 2.8777 \cdot TC^2 - 2.2023 \cdot TC \tag{8}$$

The correlation coefficient is 0.98 for 71 bins (cloud cover values of 0.0, 0.01, and 0.70 were excluded). Using Eq. (8), E_0/E_c can be calculated using TC, but the variable required as input to the DYRESM-CAEDYM lake model is TC, based on observed solar radiation. Hence an iteration method was adopted to calculate cloudiness, setting an initial cloudiness value to a random value between 0.0 and 1.0. When the estimated TC of the current iteration step was <0.00001 of the previous value, we took this value to represent TC.

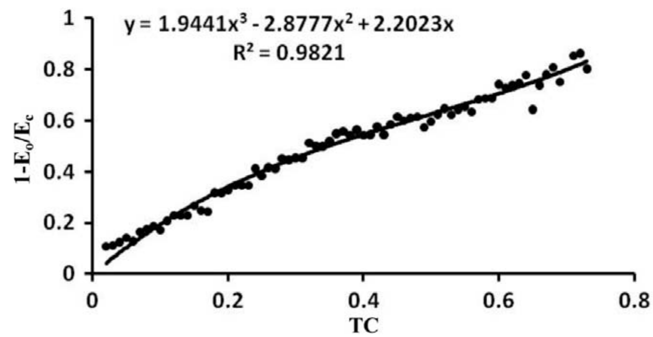

Fig. 3. Observed fractional cloud cover (TC), one minus the ratio of observed (E_0) to clear-sky (E_c) solar irradiance ($1 - E_0/E_c$), and the regression between TC and ($1 - E_0/E_c$). The 15 black dots are values of ($1 - E_0/E_c$) and the solid line is the regression of ($1 - E_0/E_c$) on TC.

3.3. Model validation

In order to test the accuracy of the regression equation for estimating cloud cover, we downloaded the solar radiation and cloud cover data from the same database operated by NIWA for the period 1 March–30 April 2009 (ordinal date from 60 to 120). Eq. (8) was then adopted to estimate total cloud cover using the iteration method described above. A comparison of observed and predicted TC is shown in Fig. 4. The simulations and the observations show reasonable agreement ($r = 0.86$, RMSE = 0.10 and $n = 61$) with similar trends (Fig. 4. In order to test the model's applicability to other sites, we validated it using data for Queenstown, South Island of New Zealand for the same period (1 March – 30 April 2009) from the same source. The model captured the pattern of variation

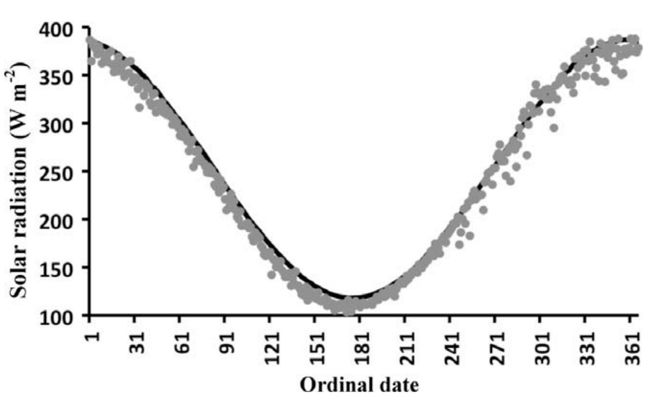

Fig. 2. Peak value of solar radiation for each day of the year (1–366) derived from observed daily data from 15 November 1991 to 20 February 2009 (gray dot) and simulated solar clear sky 10 radiation using Bird's model (black line).

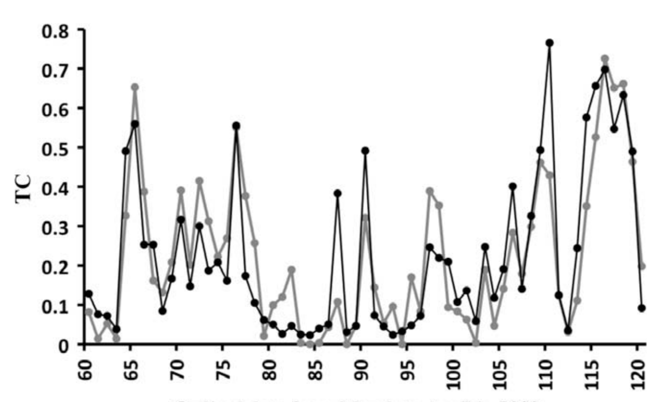

Fig. 4. Comparison between observed TC (black) and estimated TC (grey) at Lake Rotorua.

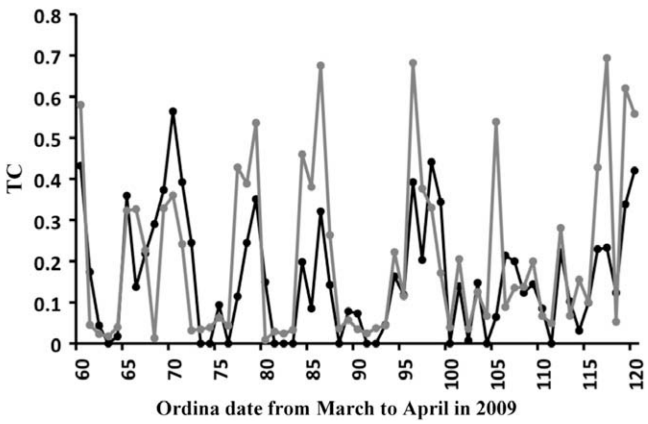

Fig. 5. Comparison between observed TC (black) and estimated TC (grey) at Queenstown.

but there was a slightly greater difference between the simulated and observed values when compared to Lake Rotorua simulations (Fig. 5, $r = 0.67$, RMSE = 0.16 and $n = 61$). The accuracy of this validation of cloud cover at the two sites suggests that this method of total cloud cover estimation could then be incorporated into DYRESM-CAEDYM for water temperature simulation based on observed short-wave solar radiation.

4. Discussion

Ineichen (2006) considered that atmospheric turbidity has the greatest effect on accuracy of solar models based on a comparison of eight clear-sky broadband models and using 16 independent data sets. Gregg and Carder (1990) suggested that air mass type, visibility and ozone concentration are the most important parameters in these solar models. In Bird's model, which was applied in this paper, the air mass changes with solar zenith and is only dependent on the local latitude, longitude and time. In our study, monthly ozone data were obtained from NOAA. The peak value of monthly ozone is in October and the trough value is in March. It keeps increasing from March to October and decreasing from October to December. The simulated clear-sky solar radiation from March to October agrees well with the observed values, but they are sometimes lower than the observations after October. That suggests that this model has low sensitivity to ozone as the ozone increase from March to September does not have a significant impact on the simulated irradiance.

The cloud cover model was established statistically based on a cubic polynomial regression between observed solar radiation and cloudiness. Although the form of the equation differs from other models (Kasten and Czeplak, 1980; Davis, 1995; Kim and Hofmann, 2005), we note that there has not been a universal equation expressing this relationship and that simple exponents to relate TC to E_0/E_c have taken values of 3.4 (Kasten and Czeplak,1980), 3.0 (Laevastu, 1960), 2.854 (Davis, 1995), 2.0 (Antoine et al., 1996), and 0.5 (Dobson and Smith, 1988); see summaries by Kim and Hofmann (2005). The different equation forms and exponent values expressing the dependence of E_0/E_c on TC suggest the relationship might differ between observation sites. Different climatic factors (e.g., atmospheric circulation, ozone and water vapour pressure), observational errors and analytical techniques may collectively contribute to these differences.

Accurate cloudiness input data to DYRESM-CAEDYM will help to improve the accuracy of water temperature simulations when there are not direct measurements of total or net long-wave radiation. Water temperature is a critical variable for lake dynamics due to its indirect influence on water column stratification and the resulting effect on biogeochemical rates (e.g., growth and respiration rates of biota). Therefore, an accurate heat budget, including improved representation of cloudiness developed in this paper, will help to improve the performance of DYRESM-CAEDYM in predicting water temperature and the resultant interactions between the physical and biochemical processes in aquatic ecosystems. In the future work, we will test how efficient of this cloud cover estimation model is in improving water temperature simulation with DYRESM.

Acknowledgements

We would like to thank the three anonymous reviewers for their valuable comments and Ben Liley from NIWA of New Zealand for providing all the aerosol optical depth data and Chris MacBride from the University of Waikato for his English correction. The project was supported by grants from the New Zealand Foundation of Research Science and Technology (UOWX0505) and by the National Natural Science Foundation of China (NSFC-40730529, 40871095, 40701136), Chinese Academy of Sciences (KZCX1-YW-14), Jiangsu Science and Technology Department (SBK20081090) and State Key Laboratory of Lake Science and Environment (20084117417492). We also acknowledge support from Environment Bay of Plenty.

References

Antoine, D., Andre, J., Morel, A., 1996. Oceanic primary production 2. Estimation at global scale from satellite (coastal zone color scanner) chlorophyll. Global Biogeochemical Cycles 10, 57–69.

Bird, R.E., Riordan, C., 1986. Simple solar spectral model for direct and diffuse irradiance on horizontal and titled planes at the earth's surface for cloudless atmospheres. Journal of Climate and Applied Meteorology 25, 87–97.

Bird, R.E., Hulstrom, R.L., 1981. A Simplified Clear Sky Model for Direct and Diffuse Insolation on Horizontal Surfaces. Technical Report No. SERI/TR-642-761, Solar Energy Research Institute, Golden, CO.

Bird, R.E., 1984. A simple spectral model for direct normal and diffuse horizontal irradiance. Solar Energy 32, 461–471.

Calbo, J., 2001. A method for sky-condition classification from ground-based solar radiation measurements. Journal of Applied Meteorology 40, 2193–2199.

Davis, R., 1995. Comparison of modelled to observed global irradiance. Journal of Applied Meteorology 35, 192–201.

Dobson, F., Smith, S., 1988. Bulk models of solar radiation at sea. Quarterly Journal of Royal Meteorological Society 114, 165–182.

Gregg, W., Carder, K., 1990. A simple spectral solar irradiance model for cloudless maritime atmospheres. Limnology and Oceanography 35, 1657–1675.

Gul, M., Muneer, T., Kambezidis, H., 1998. Models for obtaining solar radiation form other meteorological data. Solar Energy 64, 99–108.

Gal, G., Imberger, J., Zohary, T., Antenucci, J.P., Anis, A., Rosenberg, T., 2003. Simulating the thermal dynamics of Lake Kinneret. Ecological Modelling 162P, 69–86.

Hamilton, D.P., Schladow, S.G., 1997. Prediction of water quality in lakes and reservoirs. Part I – model description. Ecological Modelling 96, 91–110.

Ineichen, P., 2006. Comparison of eight clear sky broadband models against 16 independent data banks. Solar Energy 80, 468–478.

Karalis, J.D., Pissimanis, D.K., Notaridou, V.A., 1982. Estimation of global, direct and diffuse solar radiation in Athens under clear sky conditions. Theoretical and Applied Climatology 31 (4), 369–377.

Kasten, F., Czeplak, G., 1980. Solar and terrestrial radiation dependent on the amount and type of cloud. Solar Energy 24, 177–189.

Kim, H., Hofmann, E.E., 2005. Evaluation and derivation of cloud-cover algorithms for calculation of surface irradiance in sub-Antarctic and Antarctic environments. Antarctic Science 17 (1), 135–150.

Laevastu, T., 1960. Factors affecting the temperature of the surface layer of the sea. Commentativeness Physico-Mathematicae 25, 1–136.

Marion, W., George, R., 2001. Calculation of solar radiation using a methodology with worldwide potential. Solar Energy 71 (4), 275–283.

Muneer, T., Gul, M., 2000. Evaluation of sunshine and cloud cover based models for generating solar radiation data. Energy Conversion and Management 41, 461–482.

Oltmans, S., Clark, M., Evans, R., Hackathorn, E., Harris, J., Johnson, B., Koenig, G., O'Neill, M., Quincy, D., Vömel, H., 2009. Ozone and water vapor. <http://www.esrl.noaa.gov/gmd/publications/annrpt24/411.htm> (accessed 15.11.09).

Richards, K., Sullivan, G.D., 2009. Estimation of cloud cover using colour and texture. <http://www.bmva.org/bmvc/1992/bmvc-92-045.pdf> (accessed 13.02.09).

Romero, J.R., Antenucci, J.P., Imberger, J., 2004. One- and three-dimensional biogeochemical simulations of two differing reservoirs. Ecological Modelling 174, 143–160.

Schladow, S.G., Hamilton, D.P., 1997. Prediction of water quality in lakes and reservoirs: part II – model calibration, sensitivity analysis and application. Ecological Modelling 96, 91–110.

Sospedra, F., Caselles, V., Valor, E., Dibella, C., Coll, C., Rubio, E., 2004. Night-time cloud cover estimation. International Journal of Remote Sensing 25 (11), 2193–2205.

Tennessee Valley Authority, 1972. Heat and Mass Transfer Between a Water Surface and the Atmosphere. Water Resources Research Laboratory Report 14, Report No. 0-6803.

Tuller, S.E., 1977. The relationship between precipitable water vapour and surface and humidity in New Zealand. Meteorology and Atmospheric Physics 26 (2–3), 197–212.

Yamashita, M., Yoshimura, M., Nakashizuka, T., 2004. Cloud cover estimation using multi-temporal hemisphere imageries. International Archives of Photogrammetry Remote Sensing and Spatial Information Sciences 35 (7), 826–829.

Younes, S., Muneer, T., 2007. Comparison between solar radiation models based on cloud information. International Journal of Sustainable Energy 26 (3), 121–147.